

Double-exchange model with background superexchange interactions: Phase diagrams of $\text{La}_{1-x}\text{A}_x\text{MnO}_3$ manganites

Hong Suk Yi

Pohang Superconductivity Center, POSTECH, Pohang 790-784, Korea

Jaejun Yu

Department of Physics, Sogang University, Seoul 121-742, Korea

(Received 16 January 1998; revised manuscript received 22 May 1998)

The phase diagram of the double exchange model for manganites with ferromagnetic Hund coupling and antiferromagnetic superexchange coupling between t_{2g} electrons is investigated by using Monte Carlo methods in low dimensions. Extensive calculations are performed for the one- and two-dimensional lattice model where the localized spins of t_{2g} electrons are treated as classical spins. While the results for the model with no antiferromagnetic superexchange interaction are in good agreement with the recent work by Dagotto and co-workers, the regions of phase separations are found to occur both at large and low electron densities in the phase diagram with background superexchange couplings. In addition, it is noted that the ground state is changed from ferromagnetic to antiferromagnetic state for the larger antiferromagnetic superexchange interaction at quarter filling. [S0163-1829(98)08541-5]

The doped manganite compounds $R_{1-x}\text{A}_x\text{MnO}_3$ (where $R = \text{La, Pr}$; $A = \text{Sr, Ca, Ba}$)¹ have been a focus of recent studies due to the potential applicability of the very large negative magnetoresistance. While the parent compound, LaMnO_3 , is substantially distorted from the cubic perovskite structure due to the strong Jahn-Teller interaction,^{2,3} the ground state is A -type antiferromagnetic (AF), which is attributed to the cooperative interactions of orbital ordering and superexchange interactions.⁴ Although small in its magnitude, the superexchange interactions among localized t_{2g} electrons of Mn ions seem to play a crucial role in the AF ordering of LaMnO_3 . Doped with divalent cations such as alkaline-earth elements Ca, Sr, and Ba, $\text{La}_{1-x}\text{A}_x\text{MnO}_3$ becomes ferromagnetic (FM) metal for the doping range of $0.2 \leq x \leq 0.5$.⁵ For a small hole doping range of $x \leq 0.2$, neutron scattering^{2,6} and NMR (Ref. 7) experiments reveal coexisting AF and FM diffraction peaks, which is interpreted as an appearance of the weak ferromagnetism of a canted phase. For a stable canted AF phase a theoretical model was suggested by de Gennes based on a molecular field approximation of double exchange (DE) Hamiltonian with a contribution from the superexchange interaction.⁸

Recently Dagotto and co-workers⁹ obtained a phase diagram of the FM Kondo lattice model in one, two, and ∞ dimensions based on the results of numerical calculations by assuming the localized t_{2g} electron spins to be classical and neglecting the degeneracy of e_g orbitals. From their results, particularly surprising was an observation of the presence of the phase separation (PS) between hole-poor AF and hole-rich FM regions as well as a short-range incommensurate (IC) correlations in the weak Hund coupling. Recent theoretical studies,¹⁰ however, suggested a possible instability of a canted phase over the PS with some interaction parameters. Indeed, such a PS has been suggested to occur in the strongly correlated systems such as high- T_c superconductors.¹¹

Although the AF superexchange interaction, i.e., J_{AF} , was suggested to be one of the key factors in describing the

magnetic properties in manganites,¹³ its role has not been seriously considered yet. In fact, while a typical value for the Hund coupling is $J_H \approx 1$ eV, the J_{AF} is estimated^{4,12,13} to be in order of $J_{AF} \approx 0.01$ eV. Although J_{AF} is order-of-magnitude smaller than the hopping integral $t \sim 0.1$ eV, if we consider the polaronic band narrowing effects at low temperature, the role of J_{AF} can be relatively significant. Therefore, a detailed investigation of the magnetic correlations with respect to J_{AF} is necessary for the understanding of the physical properties of doped manganites.

In this report, we present results of our extensive study on the phase diagram of the DE model for $\text{La}_{1-x}\text{A}_x\text{MnO}_3$ with J_{AF} by using Monte Carlo techniques. A phase diagram for the change of the J_{AF} with a large Hund coupling at low temperature is investigated and the various results on spin correlations are presented. In the phase diagram with J_{AF} , regions of the PS's are found to occur at both large and small doping limits. In addition, it is found that the ground state is changed from the FM to the AF state for a larger J_{AF} at quarter filling.

In order to study the phase diagram of the DE model with J_{AF} , we start with a single band Hamiltonian with the FM Hund coupling and the AF superexchange interaction, i.e., J_{AF} ,

$$H = - \sum_{\langle ij \rangle, \sigma}^L (t_{ij} c_{i\sigma}^+ c_{j\sigma} + \text{H.c.}) - J_H \sum_{i,ab}^L \vec{S}_i \cdot \vec{\sigma}_{ab} c_{ia}^+ c_{ib} + J_{AF} \sum_{\langle ij \rangle}^L \vec{S}_i \cdot \vec{S}_j, \quad (1)$$

where $\vec{\sigma}_{ab}$ is the Pauli matrix for the conduction electron spins and \vec{S}_i represents the localized spin of t_{2g} electrons.

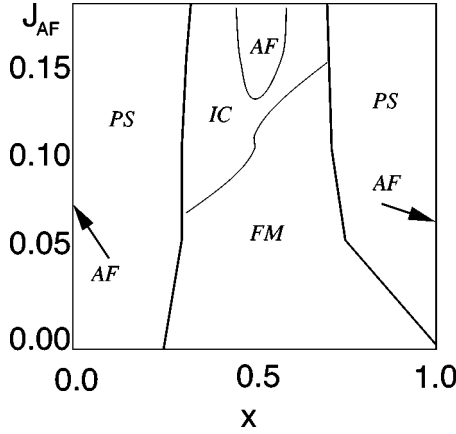


FIG. 1. Phase diagram of the DE model with a fixed value of $J_H=8t$ as a function of the superexchange interaction J_{AF} and hole doping x . The notation AF, PS, FM, IC denotes regions with antiferromagnetism, phase separation, ferromagnetism, and incommensurate regions, respectively.

The operator $c_{i\sigma}$ ($c_{i\sigma}^+$) annihilates (creates) a conduction electron with spin σ at the site i . The first term represents an effective hopping integral of e_g conduction electrons between the nearest-neighbor Mn sites. $J_H>0$ is a FM Hund coupling of e_g conduction electrons to the local spins of t_{2g} electrons. L is the system size.

To perform Monte Carlo simulations of the model Hamiltonian given in Eq. (1), we treat the localized spin \vec{S}_i as a classical spin $\vec{S}_i=|\vec{S}_i|(\sin\theta_i\cos\phi_i\hat{x}+\sin\theta_i\sin\phi_i\hat{y}+\cos\theta_i\hat{z})$ with $|\vec{S}_i|=3/2$. Then, for a fixed configuration of spin angles $\{\theta_i, \phi_i\}$, this Hamiltonian represents nothing but a system of noninteracting electrons moving in an external field of background spin configurations. By performing the diagonalization of the $(2L\times 2L)$ Hermitian matrix for each given spin configuration $\{\theta_i, \phi_i\}$, we obtain the $2L$ eigenvalues denoted by ϵ_α , i.e., $\epsilon_\alpha=\epsilon_\alpha(\theta_i, \phi_i)$. Thus the resulting partition function becomes

$$Z=\prod_i^L\left(\int_0^\pi d\theta_i\sin\theta_i\int_0^{2\pi}d\phi_i\right)\prod_{\alpha=1}^{2L}(1+e^{-\beta(\epsilon_\alpha-\mu)}). \quad (2)$$

Now, we apply a Monte Carlo integration procedure for the summation over the configuration angles $\{\theta_i, \phi_i\}$ of localized spins. The summation of the partition function was performed by using a standard Metropolis algorithm. Most of the results of calculations presented in this paper are done for the one-dimensional (1D) chain of the system size $L=24$ and 32 with periodic boundary conditions (PBC) in spatial directions. In actual Monte Carlo simulations, typically 6×10^4 initial sequences of configurations are discarded for the thermalization processes before the Monte Carlo data collections are made. We actually take $1.2\times 10^5\sim 10^6$ samples for each measurement depending on the numerical accuracies.

To obtain the phase diagram of the 1D DE model Hamiltonian with J_{AF} , we performed calculations in the large Hund coupling limit of J_H/t for the DE model at different temperatures and lattice sizes. The measurements for the evolution of FM, AF, and IC phase were obtained by calculating the spin-spin correlation functions between the classi-

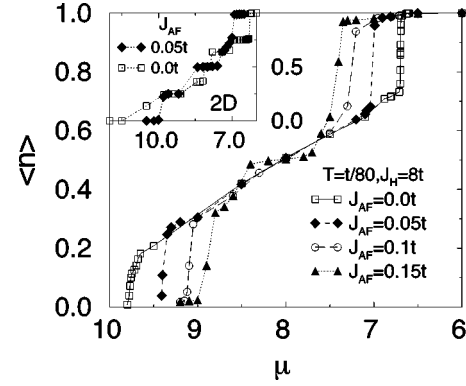


FIG. 2. The μ dependence of $\langle n \rangle$ at $J_H=8t$ and $T=t/80$ for various values of J_{AF} ranging from $J_{AF}=0.0$ to $J_{AF}=0.15t$. In the inset, a typical result of the 2D model calculations of (6×6) lattice for $J_{AF}=0.05t$ and $J_{AF}=0$ is shown.

cally treated spins of t_{2g} electrons in the low-temperature limit, e.g., $T=t/80$, as given by the spin structure factor $S(q)$,

$$S(\mathbf{q})=(1/L)\sum_{\mathbf{l},\mathbf{m}}e^{i(\mathbf{l}-\mathbf{m})\cdot\mathbf{q}}\langle\vec{S}_{\mathbf{l}}\cdot\vec{S}_{\mathbf{m}}\rangle, \quad (3)$$

where L is the system size. For $J_{AF}=0$, the strong FM correlations dominate in the overdoped region of $x\geq 0.25$ for large J_H . This FM correlation is induced by the motion of e_g conduction electrons via the strong Hund coupling J_H . In fact, our extensive calculations for the case of $J_{AF}=0$ produced the phase diagrams, spin correlations, and the PS in good agreement with the recent work by Dagotto and co-workers.⁹

By examining the spin correlation functions, we probed the phase boundaries of the model Hamiltonian with a fixed value of $J_H=8t$ but with various coupling constants J_{AF} and the electron densities $\langle n \rangle$, i.e., the hole doping level x . In Fig. 1, we present a phase diagram of the DE model with a fixed value of $J_H=8t$ as a function of J_{AF} and hole doping x . The $J_{AF}=0$ limit gives a sequence of AF, PS, and FM phases as x increases. However, as J_{AF} was turned on, a much more complicated phase structure has developed. Overall, four distinct phase boundaries of AF-PS, PS-IC or FM, and IC-AF are identified as determined by calculating the spin-spin correlations at the low temperature.

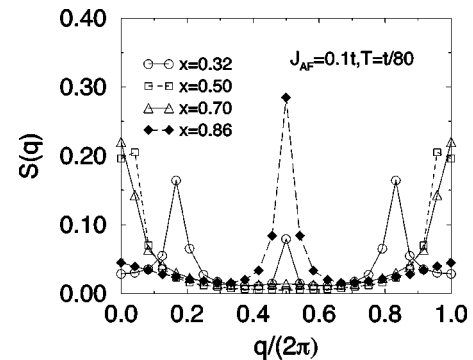


FIG. 3. Momentum dependence of $S(q)$ at $J_{AF}=0.1t$ for various values of hole dopings.

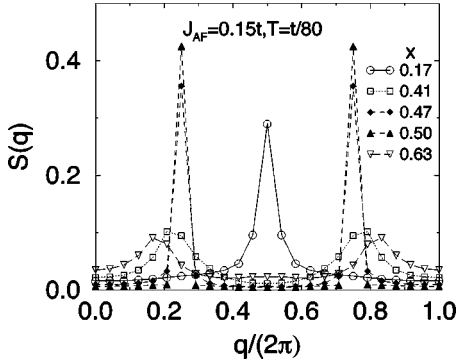


FIG. 4. Momentum dependence of $S(q)$ with $J_{AF}=0.15t$ and $T=t/80$ for the hole doping ranging from $x=0.17$ to 0.63 .

The PS regions were determined by calculating the μ dependence of the $\langle n \rangle$. In Fig. 2, we present the μ dependence of $\langle n \rangle$ at $J_H=8t$ and $T=t/80$ for various values of J_{AF} ranging from $J_{AF}=0$ to $J_{AF}=0.15t$. Although the $n(\mu)$ curves in Fig. 2 are determined at $T=t/80$, the PS regions near $x \approx 0$ and $x \approx 1$ can be clearly identified from the discontinuities of density as a function of chemical potential μ . Further, when we checked the limit of $T \rightarrow 0$, we confirmed that both knees of $n(\mu)$ curves close to $n=0$ and $n=1$ became sharp and discontinuous,¹⁴ leading to the PS region illustrated in Fig. 1. This is a clear difference from the results of $J_{AF}=0$. Especially the development of the PS region in the low electron-density limit, i.e., $x \approx 1$, for the nonzero J_{AF} is quite remarkable in comparison with the phase diagram⁹ with $J_{AF}=0$. In addition, as shown in the inset of Fig. 2, the same PS's are observed in the Monte Carlo calculations for the 2D lattice system of (6×6) lattice with various values of J_{AF} . Thus, we conclude that there is numerical evidence of PS's both in the carrier-rich and carrier-depleted region in the DE model with finite J_{AF} .

The tendency to develop a spin pattern with IC and kink structure can be easily studied by observing the behavior of $S(q)$ as densities are varied at a particular coupling. In Fig. 3, we present the momentum dependence of $S(q)$ at $J_{AF}=0.1t$ for various values of densities. A large AF peak remains even at the low electron density $\langle n \rangle=0.14$, i.e., $x=0.86$. As the electron density $\langle n \rangle$ increases, strong FM correlations develop as shown for $x=0.7$. At the quarter filling, i.e., $x=0.5$, the peak position of the $S(q)$ moves to near $q \approx 0$, i.e., $q=2\pi/L$ due to a kink which separates two FM regions with opposite spin. More details will be given elsewhere.¹⁵ However, in the low hole density region of $x \lesssim 0.32$, both the AF and IC peaks in $S(q)$ coexist. In fact, the region at $x=0.32$ is close to the phase separation region between the hole-poor AF phase and the hole-rich IC phase. While the IC phase for the small J_H with $J_{AF}=0$ was predicted by Dagotto and co-workers,⁹ it is remarkable to observe a similar IC phase derived by J_{AF} .

The strong IC spin correlations are more pronounced by the larger AF interaction. Figure 4 illustrates $S(q)$ with $J_{AF}=0.15t$ and $T=t/80$ for the hole doping ranging from $x=0.17$ to 0.63 . Similar to the case with $J_{AF}=0.1t$, the AF correlation of the model system with $J_{AF}=0.15t$ remains stable even up to $x=0.17$. Interestingly, the double-period

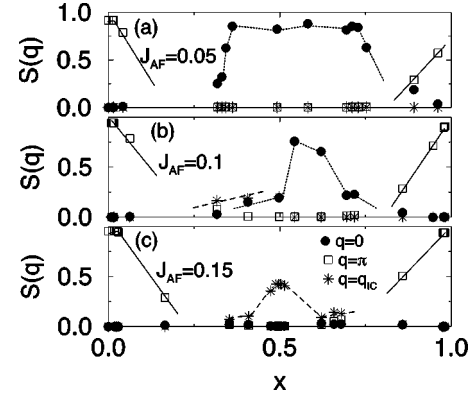


FIG. 5. Peak intensities $S(q^*)$ at $q^*=0, \pi$ and q_{IC} as a function of doping x for the various values of $J_{AF}/t=0.05, 0.1$, and 0.15 .

AF correlation, i.e., $q=\pi/2$, is found to be strong for the range of $0.45 \leq x \leq 0.55$ near the quarter filling. It means that the J_{AF} plays an important role in stabilizing the double-period AF ordering at the quarter filling. Besides the double period AF phase, the same IC spin correlations are clearly observed for the same range as in $J_{AF}=0.1t$. The peak of $S(q)$ at $q=\pi/2$ grows as temperature lowers, which indicates a possible long-range AF ordering at the quarter filling for $J_{AF} \geq 0.15t$.

To determine the phase boundaries for $J_{AF} \neq 0$ shown in Fig. 1, we plotted in Fig. 5 the peak intensities $S(q^*)$ at $q^*=0, \pi$, and q_{IC} as a function of doping x for the various values of J_{AF} . Shown in Fig. 5 are the results obtained for $J_{AF}/t=0.05, 0.1$, and 0.15 . Here, $q_{IC}=\langle n \rangle \pi$ is the q vector corresponding to the peak position of $S(q)$. It is clearly shown that the AF correlations are strongly enhanced in both limits of $x=0$ and $x=1$ as the J_{AF} is introduced. On the contrary, the FM correlations are suppressed by the presence of J_{AF} . Further, for $J_{AF} \geq 0.15t$, all the FM correlations disappear for the whole range x . Instead the IC spin correlations become dominant for $J_{AF} \geq 0.1t$.

In summary, we presented the results of our studies on the phase diagram of the DE model for manganites with FM Hund couplings and AF superexchange interactions by the Monte Carlo simulations. Through the analysis of the results obtained in the low-temperature limit, we determined the phase diagrams as a function of hole doping and J_{AF} for the large Hund coupling limit. For J_{AF} smaller than $\approx 0.1t$, the ground state remains to be FM for the hole-density range of $0.3 \leq x \leq 0.7$, and becomes AF for the half-filled region near $x \approx 0$ and the low hole density limit, i.e., $x \approx 1$. At densities near $x \approx 0$ and $x \approx 1$ with $J_{AF} \neq 0$, the systems are phase separated which may be relevant to recent experimental observations.⁵

In conclusion, it is emphasized that the ground-state properties of the DE is very sensitive to the presence of the J_{AF} . Thus, in understanding of the ground state and dynamical properties of the doped manganites, one should include such superexchange interactions properly in the model for the doped manganites. After completion of this work, we became aware of the work by Yunoki and Moreo,¹⁶ in which

they dealt with similar issues. Both results are in qualitative agreement on the phase diagram with $J_{AF} \neq 0$.

We are grateful to Professor S. I. Lee and Professor T. W. Noh for helpful discussions. This work was supported by the Korea Science Engineering Foundation (95-0702-03-01-3)

and by the Basic Science Research Institute program, Ministry of Education, 1997, Project No. 97-2415. A part of the present calculations was performed on the JRCAT Supercomputer System, which is supported by New Energy and Industrial Technology Development Organization (NEDO) of Japan.

-
- ¹S. Jin, T. H. Tiefel, M. McCormack, R. A. Fastnacht, R. Ramesh, and L. H. Chen, *Science* **264**, 413 (1994); K. Chahara, T. Ohno, M. Kasai, and Y. Kozono, *Appl. Phys. Lett.* **63**, 1990 (1993); R. von Helmolt, J. Wecker, B. Holzapfel, L. Schultz, and K. Samwer, *Phys. Rev. Lett.* **71**, 2331 (1993).
- ²E. Wollan and W. Koehler, *Phys. Rev.* **100**, 545 (1955).
- ³A. J. Millis, B. I. Shraiman, and R. Mueller, *Phys. Rev. Lett.* **77**, 175 (1996); H. Röder, Jun Zang, and A. R. Bishop, *ibid.* **76**, 1356 (1996).
- ⁴S. Ishihara, J. Inoue, and S. Maekawa, *Phys. Rev. B* **55**, 8280 (1997); A. J. Millis, *ibid.* **55**, 6405 (1997).
- ⁵P. Schiffer, A. P. Ramirez, W. Bao, and S-W. Cheong, *Phys. Rev. Lett.* **75**, 3336 (1995).
- ⁶H. Kawano, R. Kajimoto, M. Kubota, and H. Yoshizawa, *Phys. Rev. B* **53**, R14 709 (1996).
- ⁷G. Matsumoto, *J. Phys. Soc. Jpn.* **29**, 606 (1970); **29**, 615 (1970).
- ⁸P. G. de Gennes, *Phys. Rev.* **118**, 141 (1960).
- ⁹S. Yunoki, J. Hu, A. Malvezzi, A. Moreo, N. Furukawa, and E. Dagotto, *Phys. Rev. Lett.* **80**, 845 (1998); E. Dagotto, S. Yunoki, A. Malvezzi, A. Moreo, J. Hu, S. Capponi, D. Poilblanc, and N. Furukawa, *Phys. Rev. B* **58**, 6414 (1998).
- ¹⁰E. L. Nagaev, *Phys. Status Solidi B* **186**, 9 (1994); D. P. Arovas and F. Guinea, *Phys. Rev. B* **58**, 9150 (1998); M. Kagan, K. Khomskii, and M. Mostovoy, cond-mat/9804213 (unpublished).
- ¹¹V. J. Emery, S. A. Kivelson, and H. Q. Lin, *Phys. Rev. Lett.* **64**, 475 (1990); V. J. Emery and S. A. Kivelson, *Physica C* **209**, 597 (1993); U. Löw, V. J. Emery, K. Fabricius, and S. A. Kivelson, *Phys. Rev. Lett.* **72**, 1918 (1994); S. Haas, E. Dagotto, A. Nazarenko, and J. Riera, *Phys. Rev. B* **51**, 5989 (1995).
- ¹²T. G. Perring, G. Aeppli, Y. Moritomo, and Y. Tokura, *Phys. Rev. Lett.* **78**, 3197 (1997).
- ¹³P. Horsch, J. Jaklic, and F. Mack, cond-mat/9708007 (unpublished).
- ¹⁴We thank Dr. S. Yunoki for his comment on the possible temperature dependence of $n(\mu)$.
- ¹⁵H. Yi and J. Yu (unpublished).
- ¹⁶S. Yunoki and A. Moreo, *Phys. Rev. B* **58**, 6403 (1998).